Assessment of tunnels stability in the Maya archaeological area of Copán, Honduras

Emilio Bilotta[1*], *Alessandro* Flora[1], *Paulo* Lourenço[2], and *Felipe* Pires[2]

[1]University of Napoli Federico II, Naples, Italy
[2]University of Minho, Azurém, Guimarães, Portugal

Abstract. Copan is an important heritage site known by its preserved Maya ruins and recognized by UNESCO as a World Heritage Property since 1980. To investigate and understand the site development, extensive archaeological tunnels were excavated in the earthen fills of the temples in the twentieth century. Archaeologists found a series of superimposed temples, built one upon another, in a very complex chronological sequence and spatial disposition. Even though the tunnels were initially excavated in the earthen fill without putting in place any supporting structure, masonry lining was applied in parts of the tunnels years after they were excavated, in areas that suffered local collapses. Thick walls were built, forming tunnels about 1.0 m wide and 2.0 to 3.0 m high. The excavated soil is unsaturated, and thus has a strength depending on its water content and suction. Since most of the observed collapses take place during raining events, the effect of the change of the saturation degree on tunnels stability was investigated with numerical analyses. As typical in numerical simulations, the positive effects of desaturation were considered in this work through a simplified approach, introducing an 'apparent cohesion' depending on the soil water content. The outcomes indicate that in order to ensure sufficient safety margins in the tunnels, water content within the soil mass close to the tunnels, in critical sections, should be carefully monitored, and drainage in the lined sections should be ensured to avoid direct water pressure on the lining.

1 Introduction

The acropolis of Copán is created in a man-made earth fill that makes the core of the historic pyramids at the site. The embankment was made of compacted soil and rubble and therefore unsaturated. Several buried structures were rediscovered by archaeologists within the embankment by excavating horizontal underground passageways. These tunnels have an irregular pattern, with sharp changes in direction and depth when buried structures were found. Usually, the tunnels run aside substructures and foundation walls [1]. A few of them deepen to reach older stratifications of the monumental compound.

The paper addresses the stability of the tunnels under the Hieroglyphic Stairway Temple, at the northern part of Copán's Acropolis, that is the most important one in the site. Further understanding on the expected mechanical behaviour of these tunnels is the main goal of the work herein presented, to provide a preliminary assessment of their stability. This would help to implement protective actions needed to improve the safety conditions of the temple [2].

A review of all the available information allowed to define the geometrical configuration of tunnels and to obtain the mechanical characteristics of the materials. Hence, numerical analyses of tunnel stability were carried out on typical cross sections using the FE software Plaxis 2D [3].

2 The archaeological area of Copán

2.1 The site

In the western highlands of Honduras arises the ancient pre-Colombian settlement of Copán. This is a city-state prospered during the Classic Maya period, from the V to the IX century. After hundreds of years of abandonment, the archaeologists rediscovered the site in the XIX century. The so-called Main Group is the most known compound of the site, with its northern part marked by the low-level plazas, and its southern part constituted by the Acropolis. One of the most famous pieces of stonework in this compound is the Hieroglyphic Stairway (Figure 1), with the longest known Maya hieroglyphic text [4]. The Copán river changed its course along the centuries, thus destroying part of the Acropolis [5]. A river cut, known nowadays as "*corte*", slowly formed and exposed ancient layers of buried buildings. The visible

* Corresponding author: bilotta@unina.it

monuments and courtyards are just the latest of a series of additions made over the centuries, since each new king of the dynasty added a built layer on the top of the previous one [6].

Since pyramids were periodically enlarged, a series of complete but smaller pyramids, buried inside the last one, were revealed upon excavation.

Fig. 1. Picture of the Hieroglyphic Stairway Court, with the temple at right and part of the Ball Court at left – photo by Linda Schele [7].

A typical erection sequence was followed each time the structure was enlarged: first, the ancient superstructure (i.e. a building in use) was dismantled saving the recovered materials for reuse [8]; then, the base of the pyramid was widened by creating a lateral substructure around the ancient one and a new, and usually larger, superstructure was built over. Sometimes levelling platforms were built. Superstructures were generally made with three-leaf masonry walls: the external leaves are made of dressed tuff stones and the core is infilled by a sort of "concrete" [9]. Instead, a mix of wet-laid earth and stone fillings, contained by outer masonry walls, was used for substructures [10].

2.2 The tunnels

The first tunnels under the Acropolis were excavated to permit the archaeological investigation in the 1930's. More complex tunnelling started in the 1980's from the "*corte",* using the exposed layers as references (Figure 2).

Fig. 2. A view of different entrances to tunnels in the Acropolis archaeological cut in 1989 [11].

A 4 km long and complex tunnel system was created within the monumental compound, allowing extraordinary archaeological discoveries that provided the most comprehensive information on the origins and development of a Classic Maya complex [12]. UNESCO listed the site as World Heritage Property in 1980 [13] for its outstanding architectural value.

Although most of the tunnels are apparently stable, local collapses have required actions to ensure safe conditions for researchers and visitors, and to preserve the undiscovered archaeological heritage. In addition, the changing environmental conditions in the tunnels are leading in some cases to the deterioration of valuable decorations. Therefore, a strategic plan was initiated by the Copan Acropolis Tunnel Conservation Program of Harvard University [12], defining investigations, analyses, and interventions to be carried out in stages. In this framework, an important task was to assess the stability conditions of the tunnels from the available information, such as the geometric shape and position of the tunnels.

This paper addresses the stability of the tunnels under the Hieroglyphic Stairway Temple, in the northern part of the Acropolis (Figure 3a). Here the tunnels were excavated through Esmeralda (Figure 3b), a large embankment built around 700 AD, that would later become the supporting platform for the Hieroglyphic Stairway Temple [1].

The tunnels' network was excavated in most part immediately above the barro layer, in-to a layer of dark reddish-brown earth (*tierra café oscuro*) mixed with construction debris, river cobbles and broken lime plaster [12]. This is a clayey silty sand with gravel. However, assuming that the larger gravel or boulder inclusions are floating in the finer matrix, the mechanical behaviour of this layer corresponds to that of a sand with fines. The uppermost and outer part of the earth fills, the most recent one to be put in place, is made of a fine yellow sand (*girún)*. This sand was used to refine the oldest temples and to complete the latest structures such as Esmeralda, the platform under the Hiero-glyphic Stairway Temple [12]. Most tunnel stretches excavated inside the *girún* layer needed to be supported at a later stage with a stone masonry lining or suffered local collapses that required them to be back-filled.

Data about tunnel position under the Hieroglyphic Stairway Temple, their internal shape, and the presence of lining, sometimes being parts of original Maya structures, were gathered by three-dimensional

survey. Hence, four typical transverse sections were identified to carry out a parametric numerical analysis of their stability conditions (Figure 4). T1 and T2 identify the "as excavated" tunnel sections, where no lining was applied to the walls; T3 and T4 those "structurally consolidated", that were supported by thick masonry walls as lining, at a later stage. Sections T1 and T3 are fully inside the fill material, while T2 and T4 are sections of tunnel excavated adjacent to buried structures. The dimensions vary within each type but, in general, tunnels are small, serving as pathways for the archaeologists, having an average width of about 1.0 m and a height rang-ing from 2.0 m to 3.0 m. Table 1 provides the statistical information obtained from the 3D survey.

The distance between tunnels and external surfaces is represented in Figure 4 by R_{min}. This is measured from the axis at the base of the tunnel to the nearest ground surface.

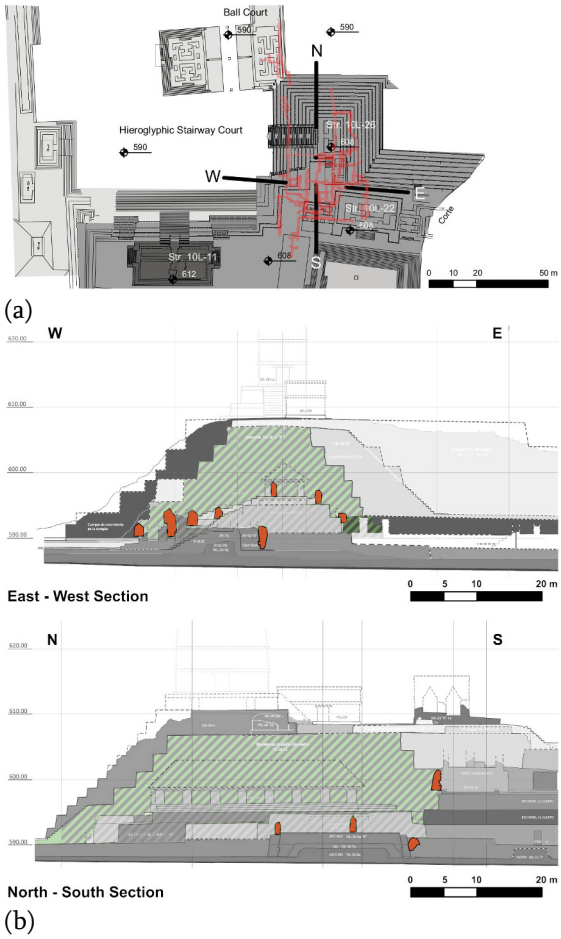

Fig. 3. (a) detail of the Acropolis plan showing the extension of currently open tunnels under the Hieroglyphic Stairway Temple (in red); (b) Sections showing the approximate positions of tunnels (in red) and the green hatch of the Esmeralda volume – adapted from C. Rudy Larios' PAAC drawings [14].

The full length of the tunnels and the range of distance to the outside surface are summarized in Table 2. Here the surface is classified as sloped or horizontal. The slope of the stepped ex-ternal surfaces of the pyramid-like structures is about 45º.

In total, about 360 m of tunnels can be found under the Hieroglyphic Stairway Temple. About 50% of the total length of these tunnels have a T3 section, while the other three sections are equally distributed (Table 2).

Collapses often occurred at the interface between lined and unlined tunnels or in unlined tunnels, as shown in the photos of Figure 5.

3 Soil behaviour

3.1 Effect of partial saturation on soil shear strength

The stability of tunnels depends on their geometrical features, on the ground cover above, on the mechanical behaviour of soil, on the lining properties and on the excavation procedure. In this study, the geometrical parameters of Copán tunnels as well as their excavation and construction procedures were known. Instead, the soil mechanical properties and those of the stone lining, where present, could be only estimated from literature, for a preliminary screening of current conditions.

It is worth noticing that the earth fills, where tunnels have been excavated, were made of compacted soil and rubble (with the tools and knowledge available in the Maya period) and they are therefore unsaturated, since the water table is assumed well below their depth, at the river level. The negative relative value of water pressure u_w, that arises in partial saturation conditions, produces a matric suction, s, that affects both soil stiffness and shear strength [15].

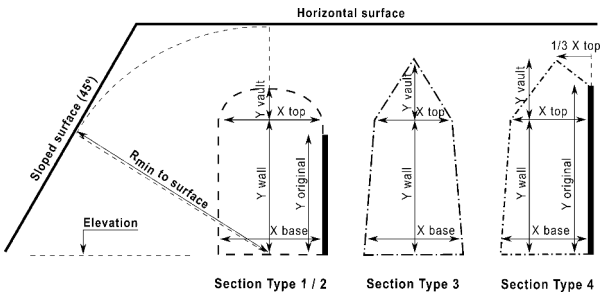

Fig. 4. Tunnel typical sections shapes: Types 1 and 2 (left), Type 3 (center) and Type 4 (right).

Table 1. Tunnel dimensions for typical sections (average – μ, standard deviation – s, and medians in meters).

Section Type	Base width		Top width		$Y_{original}$			Y_{wall}		Y_{vault}	
	μ	s	μ	s	μ	s	median	μ	s	μ	s
T1	1.3	0.2	1.2	0.1	0.0	0.0	1.1	1.3	0.3	0.6	0.2
T2	1.2	0.3	1.2	0.2	2.0	1.1	1.3	2.0	1.1	0.4	0.3
T3	1.0	0.2	0.9	0.2	0.0	0.0	1.6	1.7	0.3	0.6	0.2
T4	1.1	0.2	0.9	0.3	2.6	1.7	1.9	2.5	1.4	0.7	0.2

Table 2. Tunnels length and distance to external surface (average – μ, standard deviations – s, other values in meters)

Section Type	Total Length	R_{min} to surface					
		μ	s	Sloped		Horizontal	
				min	max	min	max
T1	51.0	15.0	7.8	4.0	4.0	15.0	20.0
T2	56.0	17.0	4.4	-	-	8.5	20.0
T3	183.5	10.6	3.8	3.0	10.0	9.5	17.0
T4	66.5	7.7	4.3	2.0	11.0	9.0	12.5

Fig. 5. Examples of local collapses at the interface between lined and unlined tunnels – left – and in an unlined tunnel – right [12].

In this work the shear strength of an unsaturated granular soil has been simply expressed as:

$$\tau = (\sigma - u_a) \cdot tan(\varphi) + (u_a - u_w) \cdot S_r \cdot tan(\varphi) \quad (1)$$

where $(\sigma - u_a)$ is the net normal stress, $(u_a - u_w)$ is the matric suction s, as defined above, S_r is the degree of saturation of the soil and φ is the effective friction angle. The second term of the second member of Eq. (1) is often designated as the "apparent cohesion":

$$c_{unsat} = (u_a - u_w) \cdot S_r \cdot tan(\varphi) \quad (2)$$

By using c_{unsat} in Eq. (1), the shear strength can be expressed according to the classical formulation of Mohr-Coulomb strength criterion. However, the apparent cohesion is not an intrinsic soil property but a state variable, depending on suction, degree of saturation and friction angle. Changes in the degree of saturation of the soil, for instance because of rain, affect the soil suction. The water retention function or soil-water characteristic curve, was estimated according to [16]:

$$S_r = \left\{ \frac{1}{ln\left[2.718 + \left(\frac{s}{a}\right)^n\right]} \right\}^m \quad (3)$$

Based on the available information on the grain-size distribution of a soil sample of the silty sand named '*girún*', the following values have been adopted: a = 46, m = 1.2 and n = 0.86 [16]. Figure 6a shows the water retention curve and Figure 6b the resulting curve expressing the relation between apparent cohesion and saturation (assuming $\varphi = 30°$).

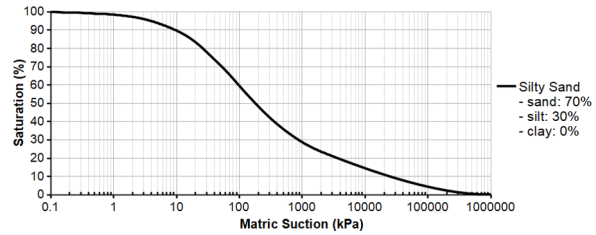

(a)

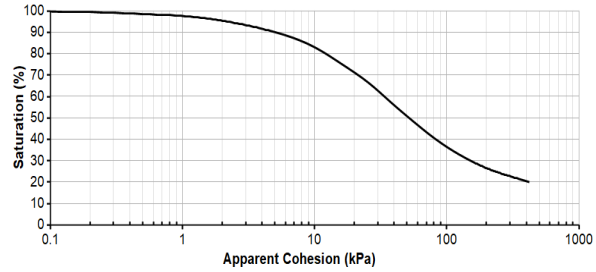

(b)

Fig. 6. Assumed SWCC and apparent cohesion versus saturation for the silty sand infill ('*girùn*').

4 Analysis of tunnel stability

4.1 Numerical model

The stability conditions of tunnels in different scenarios of water infiltration caused by rain are analysed in this section, by assuming different values of the apparent cohesion c_{unsat} related to changes of degree of saturation. This approach is widely used in engineering applications since it can be easily implemented in a "strength reduction" analysis, that is a common numerical procedure that consists in progressively reducing the original shear strength of the materials.

Plane-strain analyses were performed on simplified isolated typical section models (T1, T2 and T3), considering their minimum and maximum depths (9 and 20 m) and average values of the tunnel sizes (see Table 1). T4 was not considered because it is always more stable than T3 of similar size, thanks to the presence of an adjacent buried structure. To assess the tunnel stability conditions, the outer profile of the earth fill (see Figure 3) was ignored, and level ground conditions were assumed. The global size of the model

is large enough to permit fully development of the expected deformation patterns around tunnels at failure. For T1 sections, the ground is made of a single material ("soil" in Table 3a); in T2 sections, ancient platform walls are present at one side; T3 sections have a stiff invert: the same stiffer material was adopted in different positions in both cases T2 and T3 ("platform" in Table 3a).

The numerical model used 15-noded triangular elements with variable size since the mesh was refined where large stress concentrations or large deformation gradients were expected (minimum size of about 0.05 m at the tunnel crown, maximum size of 1.00 m at the sides and bottom of the mesh). Both horizontal and vertical displacements were restrained at the bottom of the mesh, while horizontal displacements only were prevented at its vertical sides. Porewater pressures were not generated.

Where applicable, the masonry lining was modelled using volume elements and blocks, mortar and block-mortar interfaces were smeared out in a homogeneous and isotropic continuum [17]. Two material models implemented in Plaxis library were used, the "Concrete model" and the "Mohr-Coulomb model", by adopting literature values for the relevant parameters ([18], [19], [20]), shown in Tables 3a and 3b. In the tables, f_t indicates the tensile strength, f_c indicates the compressive strength, G_t indicates the tensile fracture energy, G_c indicates the compressive fracture energy and ψ indicates the dilatancy angle.

The soil-lining interface was modelled as linear elastic, with a normal stiffness K_n = 10 GPa/m and a shear stiffness K_s = 0.05 GPa/m. The adopted normal stiffness represents a common value in masonry (e.g. [21]) and a preliminary verification indicated that the safety conditions of the cavity are not significantly sensitive to this parameter. The shear stiffness was kept extremely low to prevent shear stress transfer between the soil and the lining.

Table 3a. Parameters for "Mohr-Coulomb model" materials

	E	ν	c	γ	φ	f_t
	MPa	-	kPa	kN/m^3	-	kPa
soil	17	10	0.3	var.	30°	
platform	1000	0.3	390	17	35°	0
masonry lining (T3_Lined_Mohr-Co)	1000	0.2	390	20	35°	100

Table 3b. Parameters for "Concrete model" material

	E	ν	f_c	G_c	φ	ψ	f_t	G_t
	MPa	-	MPa	kN/m	-	-	kPa	N/m
masonry lining (T3_Lined_Concrete)	1000	0.2	1.5	2.5	35°	0°	100	15

4.2 Stress initialization

The stress distribution around tunnels has been initialized as follows: (1) a lithostatic (K_0) stress distribution is initially assumed; (2) an apparent cohesion is assigned to soil corresponding to an initial degree of saturation S_r=20% according to Eq. (2); (3) the tunnel opening is simulated by removing the corresponding soil elements; (4) the lining elements are activated, when applicable (i.e., for T3 sections); (5) the apparent cohesion, c_{unsat}, is reduced to simulate the increase of the degree saturation caused by rain, scanning the soil-water characteristic curve in Figure 6b. Hence, for each level of apparent cohesion, the stability conditions have been assessed reducing progressively the original shear strength, τ (i.e. c=c_{unsat} and tan φ), to a value τ_{red} (i.e. c=c_{red} and tan φ_{red}), that was identified as follows.

4.3 Safety factor

The safety factor of the tunnel section, SF, is defined according to the following equation:

$$SF = \frac{c}{c_{red}} = \frac{tan\,\varphi}{tan\,\varphi_{red}} \quad (4)$$

identified on a curve plotting SF as a function of the displacement of an appropriately selected node, where the calculated SF keeps constant in subsequent calculation steps.

For T3 sections the strength reduction procedure was applied only to the ground above the tunnel invert level, assuming that water infiltration takes place from above. Hence, the layer below the tunnel invert kept a stable cohesion (corresponding to the initial value of S_r).

It must be emphasized that the stability assessment has been carried out assuming an in-crease of the saturation of the soil as the sole effect of water infiltration. This is correct as long as the soil keeps its unsaturated state. When the soil approaches full saturation (implying lack of apparent cohesion and collapse of unlined tunnel sections, as shown in the next section) water pressure should be considered acting on the tunnel lining where present. However, such contribution was neglected here, assuming the tunnel boundary as "fully drained" due to the lack of a fully waterproof coating layer, that locally brings to zero the water pressure.

4.4 Results

Figure 7 plots the safety factors for the unlined section T1 and T2, at a same depth H = 20 m, for different value of apparent cohesion. This shows the effect of a side wall on the stability of the unlined section of

tunnels: for apparent cohesion values corresponding to clearly unsaturated soil conditions (S_r up to 70%), the safety factor of section with an ancient wall on one side (T2) is 10% to 30% higher than in T1 section, without the wall. However, approaching saturation the two curves converge around the value S_r = 85% (when in both sections SF=1), due to the failure of the lateral wall.

The masonry lining was installed an addition to pre-existing unlined tunnels. Hence, the configuration of the lined section T3 has been assumed as stemming from an enlargement of unlined section T1 (stage "T3_Unlined_Extrados" in calculation), followed by the installation of the masonry lining. This sequence has been reproduced in calculation. In the stage of stress initialization, prior to the stability analysis, the tunnel section was first enlarged ("T3_Unlined_Extrados"), then lined ("T3_Lined_Intrados"). The reduction of safety factor due to section enlargement has been checked and it resulted negligible. Figure 8 shows how instead the safety factors increase passing from the unlined to a lined section. The lining provides high safety margin to the tunnel, whatever the soil saturation degree, and ensures stability even in fully saturated conditions. The different constitutive models adopted for masonry ("T3_Lined_Concrete" and "T3_Lined_Mohr-Co") produce a very small difference between the corresponding curves of SF, being the former more conservative than the latter.

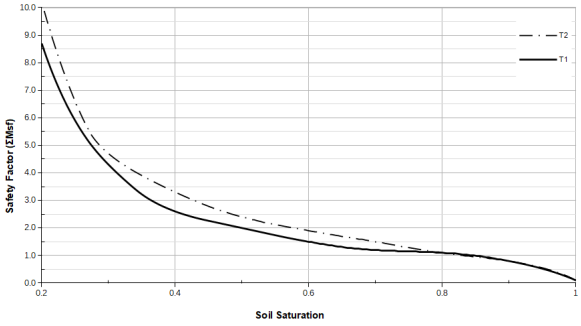

Fig. 7. Comparison of safety factors for T1 and T2 typical sections at maximum depth (H = 20 m).

All the analyses carried out on lined sections show a typical out-of-plane failure mechanism of the side walls, leading to tunnel instability. The walls bulge inwards being their top and base movements restrained, due to the masonry arch at the top and to the unchanging cohesion in the soil at the base (unaffected by a change of the saturation degree in the soil above). Would the latter condition be removed, the stability reduces drastically with the increase of saturation ("T3_Lined_UnstableBase" in Figure 8).

A sensitivity analysis on the mechanical characteristics of the lining has been carried out by varying the stiffness (E) and strength (f_c) parameters of the lining (see [14]), adopting the more conservative "concrete model" for this purpose. All these parametric calculations achieved safety factors larger than unity.

5 Conclusions

The work intended to investigate the stability of the tunnel system within the archaeological area of Copán (Honduras).

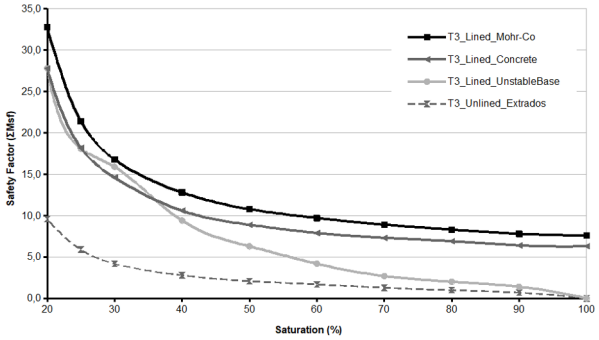

Fig. 8. Safety factors for different material models and tunnel sections and conditions as a function of the degree of saturation of soil.

The preliminary screening of the tunnel system for their stability in presence of heavy rainfall, that may increase water content and soil saturation around the tunnels, should help the site managers to undertake possible conservation actions, such as back-filling tunnels, adding masonry lining in unlined tunnels and further characterize the site.

The safety analyses that have been carried out allowed to estimate different response of lined and unlined section of tunnels to soil saturation. Unlined tunnels may collapse for a saturation degree higher than 70%, with a failure mechanism mainly consisting of a large convergence of side walls (i.e., bulging inwards). On the contrary, lined tunnels do not fail when the soil becomes saturated, as long as drainage is ensured (i.e. no water pressure develops around the lining and the tunnel base is protected).

The following recommendations can be made to permit the tunnel in the Copán site to be safely accessed:

- carry out a constant monitoring the water content in the soil around tunnels to anticipate safety issues;
- ensure drainage in the lined tunnel sections to avoid rising of water pressure on the lining;
- avoid the addition of new tunnels close to the existing tunnels.

The authors sincerely thank Laura Lacombe, Professor William L. Fash of the Department of Anthropology at Harvard University, and Corpus of Maya Hieroglyphic Inscriptions Director Barbara Fash from the Peabody

Museum of Archaeology and Ethnology at Harvard, as well as the Santander Program for the Research and Conservation of Maya Sculpture that the Fashes co-direct, and the Instituto Hondureño de Antropología e Historia for its collaborations and supervision of all research in Copan and for making available the information that provided the basis for the present article.

References

1. Sharer, R. J., Traxler, L.P., Sedat, D.W., Bell, E.E., Canuto, M.A. and Powel, C. 1999. Early Classic Architecture Beneath the Copan Acropolis, *Ancient Mesoamerica*, 10(1), 3–23.
2. Flora A. 2022. Taking care of heritage, a challenge for geotechnical Engineers. In *Geotechnical Engineering for the Preservation of Monuments and Historic Sites III (Lancellotta, Viggiani, Flora, de Silva & Mele Eds)*. 19-54.
3. Plaxis 2020. *Material Models Manual and Reference Manual - Plaxis CONNECT Edition V20.02*. PLAXIS.
4. Sharer, R.J. & Traxler, L.P. 2006. *The Ancient Maya*. 6th edn. Stanford University Press.
5. Bell, E.E., Canuto, M.A. & Sharer, R.J. 2004. *Understanding early classic Copan*. Philadelphia: University of Pennsylvania - Museum of Archaeology And Anthropology.
6. Fash, W.L. 1991. *Scribes, Warriors and Kings: The City of Copán and the Ancient Maya*. London: Thames and Hudson.
7. Schele, L. no date. *The Linda Schele Photograph Collection*. Available at: http://research.famsi.org/schele_photos.html (Accessed: 4 May 2020).
8. Abrams, E.M. 1994. *How the Maya built their world: energetics and ancient architecture*.
9. Loten, S.H. & Pendergast, D.M. 1984. A Lexicon for Maya Architecture, *Archaeology Monograph*. Toronto: Royal Ontario Museum.
10. Abrams, E.M. & Bolland, T.W. 1999. Architectural energetics, ancient monuments, and operations management, *Journal of Archaeological Method and Theory*, 6(4), 263–291.
11. Sharer, R.J., Miller J. C. & Traxler L.P. 1992. Evolution of Classic Period Architecture In The Eastern Acropolis, Copan: A Progress Report. *Ancient Mesoamerica* 3(1). 145-59. http://www.jstor.org/stable/26307232.
12. Lacombe, L., Fash, W.L. & Fash, B. 2020. *Plan for the Long-term Conservation of the Copan Acropolis Tunnels*, Report presented to the Instituto Hondureño de Antropología e Historia, October.
13. IHAH 2014. *Sitio Maya de Copán - Plan de Manejo 2014 – 2020*. Instituto Hondureño de Antropologia e Historia. Tegucigalpa.
14. Pires F., Bilotta E., Flora A. & Lourenço P.B. 2021. Assessment of Excavated Tunnels Stability in the Maya Archeological Area of Copán, Honduras, *International Journal of Architectural Heritage*, DOI: 10.1080/15583058.2021.1931730
15. Han, Z. & Vanapalli, S.K. 2016. Stiffness and shear strength of unsaturated soils in relation to soil-water characteristic curve, *Géotechnique*, 66(8), 627–647
16. Tarantino, A. & Di Donna, A. 2019. Mechanics of unsaturated soils: Simple approaches for routine engineering practice, *Rivista Italiana di Geotecnica*, (4), 5–46.
17. Lourenço, P.B. 2008. Structural Masonry Analysis: Recent Developments and Prospects, in *Proceedings of the 14th international brick and block masonry conference*. Sydney, Australia.
18. Rowe, R.K. 2001, *Geotechnical and Geoenvironmental Engineering Handbook*. Edited by R. K. Rowe. Boston, MA: Springer US.
19. Das, B.M. & Sobhan, K. 2018. *Principles of Geotechnical Engineering*. 9th ed. Boston: Cengage Learning.
20. Ghiassi, B., Vermelfoort, A.T. & Lourenço, P.B. 2019. Masonry mechanical properties, in *Numerical Modeling of Masonry and Historical Structures*. Elsevier, 239–261.
21. Lourenço, P.B. & Rots, J.G. 1997. Multisurface interface model for the analysis of masonry structures, *J. Engrg. Mech.,* ASCE, 123(7), 660-668.